Powder Technology 397 (2022) 117103

Contents lists available at ScienceDirect

Powder Technology

journal homepage: www.elsevier.com/locate/powtec

Measurement of particle adhesion force and effective contact radius via centrifuge equipped with horizontal and vertical substrates

Yasuhiro Shimada, Motohiro Tsubota, Shuji Matsusaka *

Department of Chemical Engineering, Kyoto University, Kyoto 615-8510, Japan

ARTICLE INFO

Article history:
Received 9 November 2021
Received in revised form 26 December 2021
Accepted 29 December 2021
Available online 2 January 2022

Keywords:
Centrifuge
Particle removal
Moment balance
Adhesion force
Contact radius

ABSTRACT

A centrifugal method was used to analyze and evaluate particle–surface interactions. Particles with count median diameters of 9.7, 14.5, and 32.8 μm were removed from horizontally and vertically mounted metal substrates. A point-mass model is conventionally used to analyze the forces exerted on particles during centrifugation. Conversely, in this study, a rigid-body model was employed considering the particle diameter and effective contact radius between a particle and substrate. As the moments of force exerted on the particles on the horizontal and vertical substrates were simultaneously formulated, the adhesion force and contact radius could be determined based on the particle diameter and angular velocities obtained at a given removal fraction. It was quantitatively demonstrated that as the particle diameter, relative humidity, and/or initial load increase and surface roughness decreases, the adhesion force increases. Furthermore, the contact radius increased as the particle diameter and/or surface roughness increased.

1. Introduction

Adhesiveness is defined as the ratio of adhesion to gravitational force. Particle adhesiveness significantly affects the operations performed using powders. For example, highly adhesive powders clog narrow pipes and hinder the stability of the operation as they readily form particle layers on walls. Adhesiveness increases as the particle diameter decreases for microparticles with diameters ≤100 μm. Previous studies reported that the adhesion force varies according to different particle surface properties such as moisture and static electricity [1,2]. Furthermore, the adhesion force decreases when a coating is performed using fine particles [3,4]. In addition to environmental conditions and modification of particle surfaces, various factors, such as particle diameter, surface roughness, and contact state, complicate the theoretical analysis and prediction of particle adhesion forces.

Several methods, such as the pendulum, spring-balance, centrifugation, vibration, impact, and airflow, have been proposed to measure adhesion forces [5]. In addition, the colloidal probe method using an atomic force microscope [6] and the spring-balance method using a contact needle [1] have also been investigated to measure the adhesion force directly. However, these methods cannot simultaneously evaluate multiple particles. Therefore, they are not suitable for the statistical analysis of the adhesion force and evaluation of the overall operability. The centrifugation, vibration, impact, and airflow methods can analyze the particle removal fraction by gradually increasing the external force exerted on numerous particles [5]. In particular, the centrifugation method is useful and effective because it is accurate with proper calibration and maintenance. It is also relatively easy to operate and is widely used for general purposes [7].

The centrifugation method has been used for measuring the adhesion force between particles and substrates to analyze various factors that affect the adhesion force, such as particle diameter [8–11], particle surface properties [8–11], and initial load between the particles and substrates [10]. The experimental and theoretically determined values were also compared [9,10]. Studies have been conducted wherein the substrate was not positioned such that the centrifugal force opposed the adhesion force but was sloping relative to the rotational direction [12]. However, the effects of the particle diameter and the size of the contact region were not reflected in the results as a point-mass model was used to analyze the adhesion force. Hence, it was necessary to apply moments of force based on the rigid-body model to improve the model [13]. This analysis method was successfully performed in studies where the substrate was positioned horizontally and vertically within the centrifuge [14]. We subsequently applied this method to evaluate the adhesion force, including the effects of non-spherical particles and surface roughness [5,15,16].

This study used a centrifugation method to remove particles from substrates positioned horizontally and vertically. The moments of force exerted on the particles were also analyzed in detail. Methods for obtaining the particle adhesion force and particle–substrate effective

* Corresponding author.
E-mail address: matsu@cheme.kyoto-u.ac.jp (S. Matsusaka).

https://doi.org/10.1016/j.powtec.2021.117103

Nomenclature

a	effective contact radius between particle and substrate, m
D_p	particle diameter, m
D_{p50}	count median diameter of particles, m
F	cumulative distribution function of particle diameter
F_a	adhesion force, N
F_0	initial load, N
g	gravitational acceleration, m/s^2
m_p	particle mass, kg
n	number of particles remaining in the area
n_0	initial number of particles in the area
r	centrifugation radius, m
R_a	arithmetic mean roughness, m
T	temperature, °C
η	removal fraction
θ	half-apex angle, rad
σ_g	geometric standard deviation of particle size distribution
φ	relative humidity
ω	angular velocity, rad/s

Subscripts

H	horizontal substrate
V	vertical substrate

contact radius were verified by formulating and combining the equilibria of the moments of force exerted on the particles on horizontal and vertical substrates and substituting with the measurements of two angular velocities. Additionally, the effects of particle diameter, surface roughness, humidity, and particle–substrate initial load on centrifugation were investigated.

2. Theory and calculation

2.1. Particle–wall contact

Fig. 1 presents a schematic diagram showing contact states between a particle and a wall [5]. Theoretically, a perfectly rigid sphere on a smooth wall exhibits a single point of contact [Fig. 1 (a)]. However, practical spherical particles undergo a certain deformation in the contact region. This, in turn, results in planar contact [Fig. 1 (b)]. Additionally, contact occurs at multiple points with a rough wall [Fig. 1 (c)] and/or irregularly shaped particle [Fig. 1 (d)]. There is no simple classification given the different contact states between particles and walls. However, if the contact regions are simplified as the bases of cones, particle–wall contact can be expressed based on a general-purpose model, as indicated by the broken lines in Figs. 1 (b) to (d).

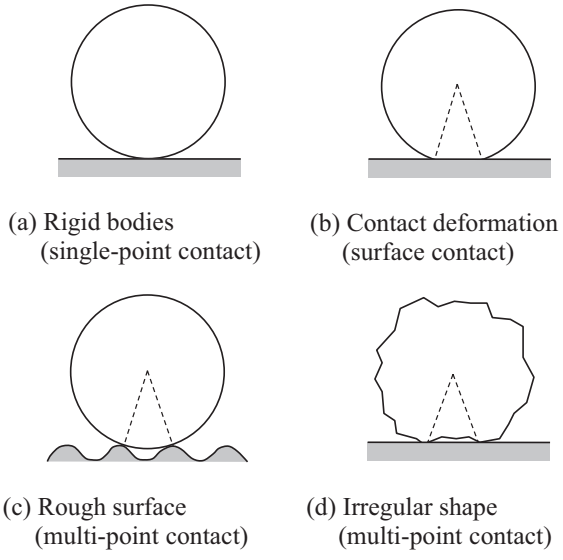

Fig. 1. Contact states between particle and wall.

2.2. Analysis of adhesion force and effective contact radius

Fig. 2 (a) shows the adhesion, gravitational, and critical centrifugal forces corresponding to the removal of a particle on a horizontal substrate based on the model described above [5]. The particle is defined as a sphere of diameter D_p, and the half-width of the contact region between the particle and substrate is defined as the half-apex angle (θ). The particle is subjected to a gravitational force of $m_p g$ in the vertical downward direction with the adhesion force (F_a) exerted in the same direction by designating the particle's mass and gravitational acceleration as m_p and g, respectively. Additionally, the particle is subjected to a centrifugal force of $m_p r\omega_H^2$ in the horizontal direction by designating the centrifugation radius as r and angular velocity as ω_H. When the half-width of the contact region between the particle and substrate is defined as the effective contact radius (a), denoted by (D_p/2) sin θ, the combined moments of force on the particle at centrifugal separation is as follows:

$$(F_a + m_p g)a = m_p r\omega_H^2 \sqrt{\left(\frac{D_p}{2}\right)^2 - a^2} \tag{1}$$

where the fulcrum is the point at the edge of the contact region. When $(D_p/2)^2$ is significantly higher than a^2, Eq. (1) approaches the following equation:

$$(F_a + m_p g)a \approx m_p r\omega_H^2 \frac{D_p}{2} \tag{2}$$

Fig. 2 (b) shows the adhesion, gravitational, and critical centrifugal forces corresponding to the removal of a particle on a vertical substrate. By assigning the angular velocity to ω_V, the combined moments of force on the particle at centrifugal separation is as follows:

$$(F_a - m_p r\omega_V^2)a = m_p g \sqrt{\left(\frac{D_p}{2}\right)^2 - a^2} \tag{3}$$

When $(D_p/2)^2$ is significantly higher than a^2, Eq. (3) approaches the following equation.

$$(F_a - m_p r\omega_V^2)a \approx m_p g \frac{D_p}{2} \tag{4}$$

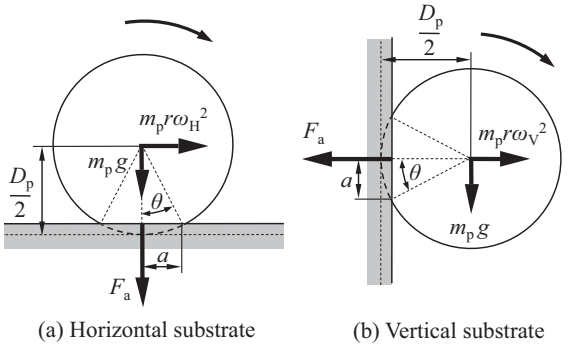

Fig. 2. Adhesion, gravitational, and centrifugal forces exerted on a particle based on a rigid-body model.

When Eqs. (2) and (4) are combined, F_a and a are as follows:

$$F_a \approx m_p \cdot \frac{(r\omega_H\omega_V)^2 + g^2}{r\omega_H^2 - g} \tag{5}$$

$$a \approx \frac{D_p}{2} \cdot \frac{r\omega_H^2 - g}{r\omega_V^2 + g} \tag{6}$$

This analysis method offers the advantage of obtaining F_a and a using two angular velocities. When $r\omega_H^2$ and $r\omega_V^2$ are significantly higher than g, Eqs. (5) and (6) can be simplified as follows:

$$F_a \approx m_p r\omega_V^2 \tag{7}$$

$$a \approx \frac{D_p}{2}\left(\frac{\omega_H}{\omega_V}\right)^2 \tag{8}$$

Eq. (7) shows that when several conditions are satisfied, the adhesion force of a particle on a vertical substrate can be determined directly from the centrifugal force.

3. Methods

3.1. Setup

Fig. 3 shows an overview of the experimental setup. The rotation axis of the centrifuge (CT15E; Eppendorf Himac Technologies Co., Ltd.) was vertical, and the control range of the rotational velocity was set between 300 and 15,000 rpm (angular velocity: 10π to 500π rad/s). The rotor was equipped with four holders incorporating horizontally or vertically fitted cells. The rotor was covered with a tight lid such that no airflow occurred inside the rotor during operation.

Fig. 4 shows the details of the disassembly cell, which was designed for particles to adhere to the sample substrate through a 10-mm circular aperture. The centrifugation radius (r) of the center of the circular aperture was 66 mm for horizontal and vertical cells. The area used for counting the number of particles was limited to a width of 1 mm.

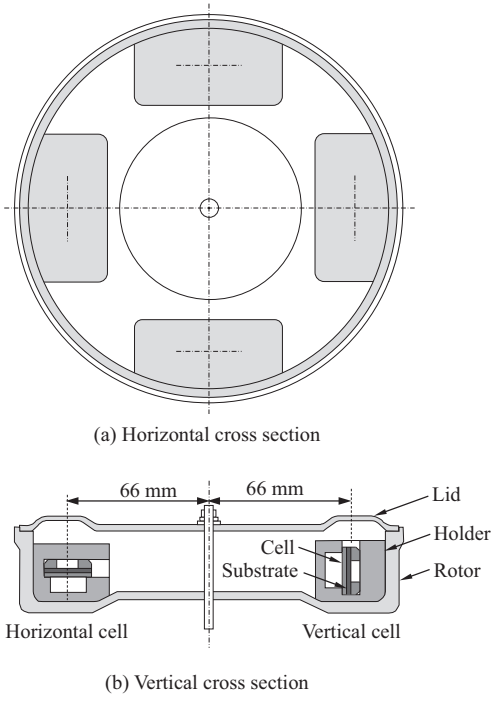

Fig. 3. Schematic diagram of the experimental setup.

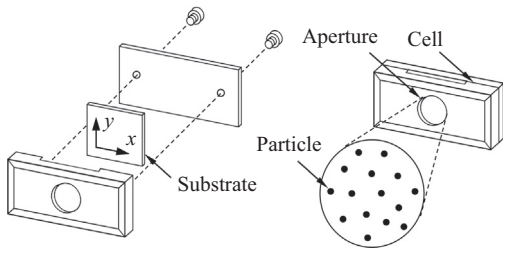

Fig. 4. Details of the cell.

Therefore, the range of the centrifugation radius of the particles was 66 ± 0.5 mm for the horizontal cell.

3.2. Sample particles

Three types of spherical particles were used as samples. All the particles were glass beads with a particle density of 2500 kg/m^3 (9000 series; Thermo Fisher Scientific, Inc.). The number-based particle size distributions, measured using an imaging method (Morphologi G3; Malvern Panalytical, Ltd.), are shown in Fig. 5. The median diameters in each sample (D_{p50}) were 9.7, 14.5, and 32.8 μm. The geometric standard deviations of the particle size distribution (σ_g) were 1.13, 1.13, and 1.08, respectively. Thus, the particle diameters were relatively uniform. The number-based median diameter of each sample was used as the representative particle diameter in the analysis [7].

3.3. Sample substrates

A and B were the two types of stainless-steel substrates with different degrees of roughness due to different surface treatments. Photographs of the substrates were obtained using a laser microscope (OLS4100; Olympus Corporation), as shown in Fig. 6. Substrate A exhibited a very smooth surface, whereas substrate B exhibited linear physical irregularities. For convenience, an axis parallel to the linear features of substrate B was assigned to the x-axis, and the corresponding orthogonal axis was assigned to the y-axis.

Fig. 7 shows cross-sections of substrates A and B obtained via laser microscopy. The arithmetic mean roughness (R_a) did not exceed 1 nm resolution in all directions for substrate A. The cross-section on the y-axis is shown where R_a was 33 nm for substrate B. It was necessary to separate and move particles along the y-axis for evaluating the effect of roughness on the centrifugal separation of particles, which was radial and vertical for the horizontal and vertical substrates, respectively.

The particles and substrates were maintained at a temperature (T) in the range of 20–25 °C and relative humidity (φ) in the range of 20–25% during storage and experiments. However, experiments were

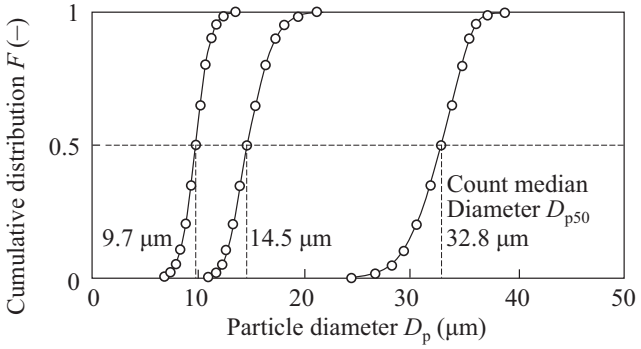

Fig. 5. Number-based particle size distribution.

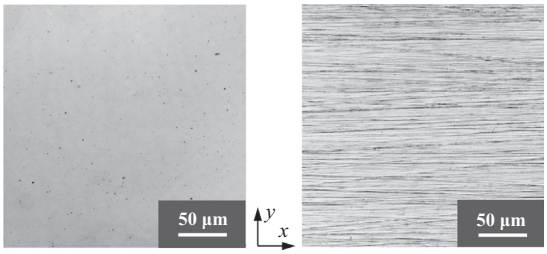

Fig. 6. Images of the substrates.

performed under a φ of 68 to 72% without altering the temperature to evaluate the effects of humidity.

3.4. Procedure for centrifugation and measurement

A minute quantity of sample particles was scattered on the substrate above the cell. The substrates were fixed, such that the surface with adhering particles was directed upward in the horizontal cells and outward in the vertical cells. The cells were detached after operating for 1 min at a specified angular velocity. The center of the circular aperture of each cell was also photographed using a microscope, and the number of particles remaining on the substrate was determined via image analysis. The centrifugation and particle number determination were repeated while increasing the angular velocity. The particle removal fraction (η) was also determined as follows:

$$\eta = \left(1 - \frac{n}{n_0}\right) \tag{9}$$

where n_0 denotes the initial number of particles in the area, and n denotes the number of particles remaining in the area.

3.5. Initial load on particles

The state of the particles remained unchanged when particles adhered to a substrate via gravitational sedimentation and the adhesion force was significantly higher than the gravitational force. However, the contact state exhibited a potential to change when the particles were pushed to the substrate by an external force [10]. The substrate was positioned with the surface of the adhering particles facing vertically inward before centrifugation. After the initial load was applied to the particles for 1 min, and centrifugation was performed with horizontal and vertical substrates.

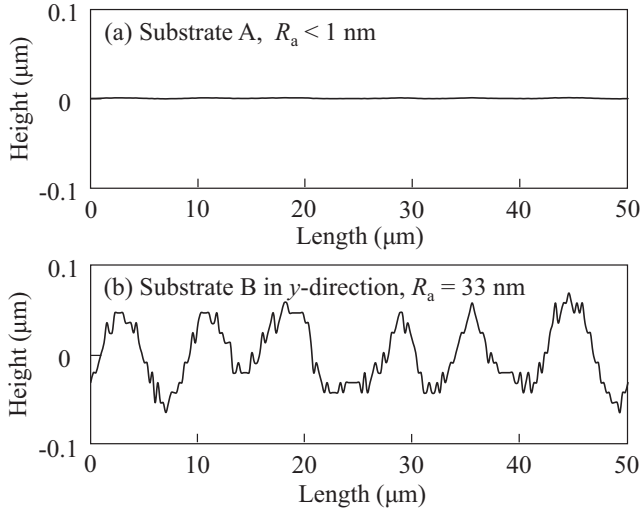

Fig. 7. Surface roughness of the substrates.

4. Results and discussion

4.1. Particles on substrate

Fig. 8 shows the photographs of particles on the substrate surface after gradually increasing the angular velocity of the centrifuge. Particles of approximately similar size adhered to the surface and were thoroughly dispersed. They were randomly detached from the substrate with increasing angular velocity.

4.2. Measurements

Fig. 9 (a) shows measurements obtained via centrifugation with particles adhering to a horizontal substrate as a parameter of particle diameter. The removal fraction increased as angular velocity increased irrespective of the particle diameter. However, the removal fraction varied significantly with particle diameter. Particles with D_{p50} = 9.7 μm were removed even with a low angular velocity, whereas larger particles with D_{p50} = 14.5 μm were not readily removed. The largest particles with D_{p50} = 32.8 μm exhibited an intermediate removal fraction. For reference, centrifugal acceleration ($r\omega_H^2$) is shown on the upper x-axis. The $r\omega_H^2$ required to remove the particles was considerably higher than the gravitational acceleration.

Fig. 9 (b) shows the measurements obtained by centrifugation with particles adhering to a vertical substrate. The removal fraction increased with increasing angular velocity. However, the angular velocity was significantly higher than for the horizontal substrate. Although most particles were removed at 100π rad/s for the horizontal substrate, approximately 50% of particles with D_{p50} = 14.5 μm remained in place even at 450π rad/s for the vertical substrate. This showed that particles were less readily removed from the vertical substrate than the horizontal substrate.

4.3. Removal fraction and centrifugal force

Fig. 10 (a) shows the removal fraction of particles adhering to the horizontal substrate as a function of the centrifugal force of the particles. The removal fraction increased as the centrifugal force increased. Furthermore, the centrifugal force required for particle removal increased as particle diameter increased. Thus, a positive correlation was observed between centrifugal force and particle diameter. The adhesion and gravitational forces on the particles associated with the horizontal substrate were exerted vertically downward. These forces increased as the particle diameter increased. Hence, the centrifugal force required to remove the particles was expected to increase.

Fig. 10 (b) shows the removal fraction of particles adhering to the vertical substrate as a function of the centrifugal force of the particles. The removal fraction increased as the centrifugal force increased. The

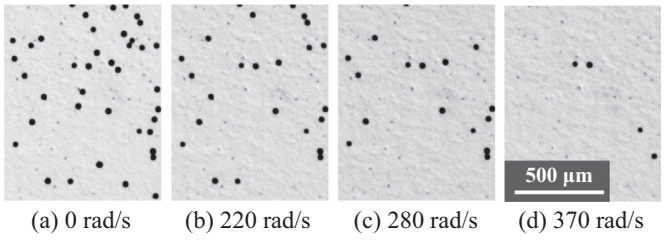

Fig. 8. Particles on the substrate for each angular velocity (D_{p50} = 32.8 μm, substrate A, vertical cell, φ = 20–25%).

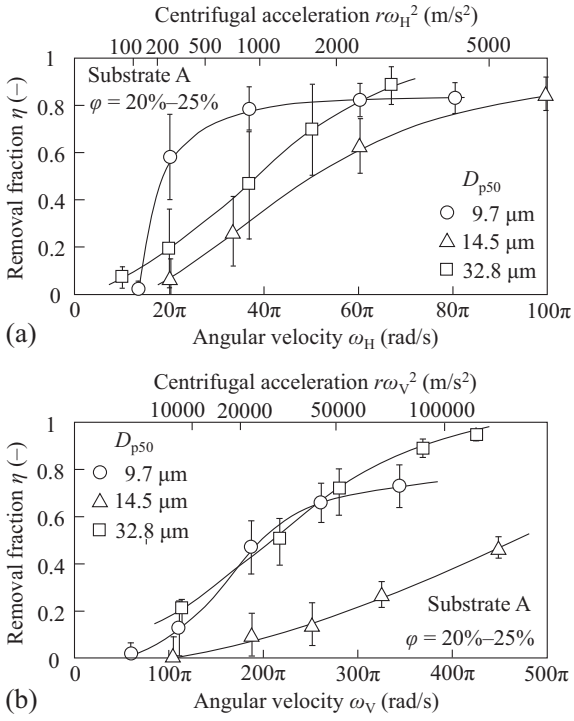

Fig. 9. Removal fraction as a function of angular velocity: (a) horizontal substrate and (b) vertical substrate.

centrifugal force required for particle removal also increased as the particle diameter increased. However, the difference in the centrifugal force required to remove particles with a D_{p50} of 32.8 and 14.5 μm was less than that with the horizontal substrate. This can be explained based on the differences in the contribution of the gravitational force. The gravitational force was more than ten times higher for D_{p50} = 32.8 μm than for D_{p50} = 14.5 μm. The gravitational force for the horizontal substrate was exerted in the same direction as the adhesion force, which aided in particle adhesion. Conversely, the gravitational force with the vertical substrate was exerted orthogonally to the adhesion force, which assisted in particle removal.

Subsequently, the ranges of centrifugal force required to remove particles from the horizontal [Fig. 10 (a)] and vertical substrate [Fig. 10 (b)] were compared. The former was considerably smaller than the latter. The point-mass model cannot explain this difference because the static friction coefficient is too small to hypothesize. Therefore, the analysis should be performed using the rigid-body model wherein particle rolling is linked to the removal mechanism. When Eqs. (2) and (4) are combined, $r\omega_H^2$ is obtained using the following equation as a function of $r\omega_V^2$ and g.

$$r\omega_H^2 \approx \left(r\omega_V^2 + g\right)\frac{2a}{D_p} + g \tag{10}$$

When $r\omega_H^2$ and $r\omega_V^2$ are higher than g and D_p is greater than $2a$, $r\omega_H^2$ is less than $r\omega_V^2$. This offers a reasonable explanation for why the centrifugal force for the horizontal substrate was less than that for the vertical substrate.

4.4. Adhesion force and effective contact radius

Fig. 11 (a) shows the adhesion force (F_a) obtained when two values (ω_H and ω_V) for the three-particle diameters were substituted in Eq. (5). Values ω_H and ω_V denote the angular velocities corresponding to the removal fraction (η) shown by the curves in Fig. 9 (a) and (b), and range of η varies with the particle diameter. F_a exhibits a positive correlation with η and corresponds to the cumulative distribution of the adhesion force represented on a number basis. Additionally, the adhesion force increased as the particle diameter increased. This was consistent with the results of previous studies [8–11].

Fig. 11 (b) shows the effective contact radius (a) obtained when two angular velocities (ω_H and ω_V) obtained by the aforementioned method were substituted in Eq. (6). Although a was not readily affected by η, it showed significant dependence on particle diameter, i.e., 0.1 to 0.2 μm for D_{p50} = 9.7 or 14.5 μm and approximately 0.5 μm for D_{p50} = 32.8 μm. An index for the contact state in all cases resulted in 0.8 to

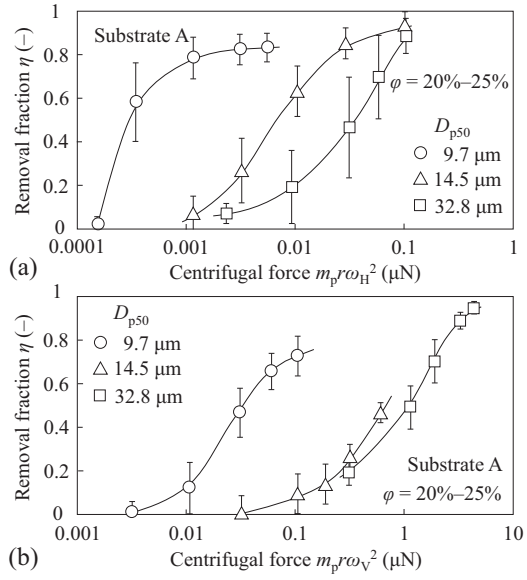

Fig. 10. Removal fraction as a function of centrifugal force: (a) horizontal substrate and (b) vertical substrate.

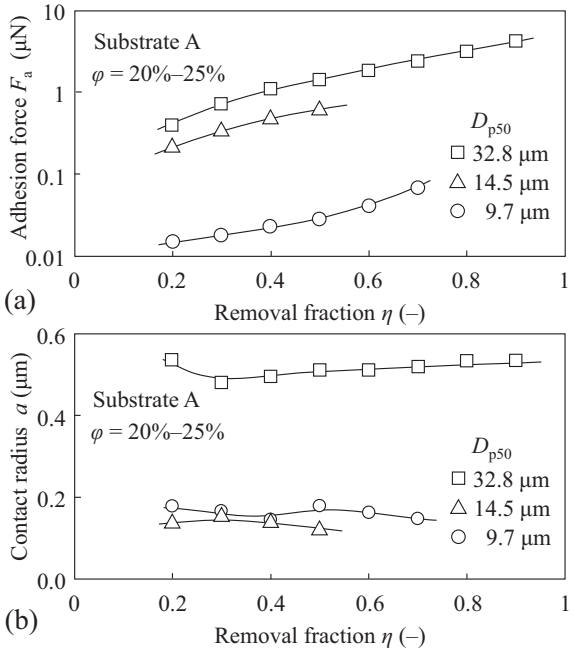

Fig. 11. Estimation as a function of removal fraction: (a) adhesion force and (b) contact radius.

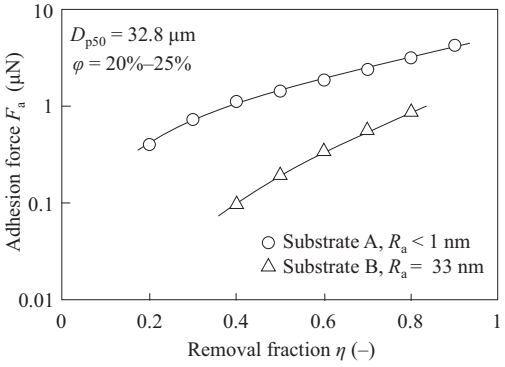

Fig. 12. Effect of substrate surface roughness on adhesion force.

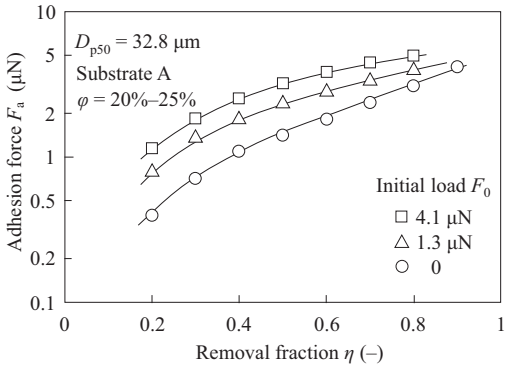

Fig. 14. Effect of initial load on adhesion force.

2.4° when switching to the half-apex angle (θ), which, in turn, corresponded to a $D_p/2a$ in the range of 24–73.

4.5. Effect of surface roughness on centrifugation

Fig. 12 shows the relationship between F_a and η for substrates A and B with different roughness values. The F_a for R_a = 33 nm was significantly less than for R_a < 1 nm. This was presumably because of an increase in the apparent distance between the contact surfaces [17,18].

The effective contact radius (a) was approximately 0.5 μm and 1.3 μm for the substrate with R_a < 1 nm and R_a = 33 nm for a particle with D_{p50} = 32.8 μm, respectively. A switch to the half-apex angle (θ) resulted in 1.7° for the former and 4.5° for the latter. Thus, it was quantitatively shown that the effective contact radius increases as the substrate surface roughness increases.

4.6. Effect of relative humidity on centrifugation

Fig. 13 shows the relationships between F_a and η under variable conditions of relative humidity (φ) during storage and experiments of particles and substrate. The F_a with φ = 68–72% was significantly greater than that with φ in the range of 20–25%. This was presumably related to the effect of the water content, i.e., liquid bridges [19]. Similar humidity dependence was obtained by the spring-balance method [1]. Thus, the results of this centrifugal method were validated.

No significant differences in the effective contact radius were found with changes in humidity in this experiment. Thus, the liquid bridge with φ of 68 to 72% was considered limited to the minute contact region between the particle and substrate.

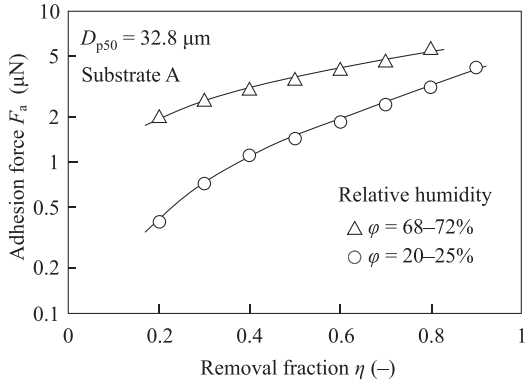

Fig. 13. Effect of humidity on adhesion force.

4.7. Effect of initial load on centrifugation

Fig. 14 shows the relationship between F_a and η when the initial load (F_0) was altered by positioning the vertical substrate in the opposite direction from the centrifugal separation and applying a centrifugal force of 0, 1.3, or 4.1 μN. Specifically, F_a increases as F_0 increases. This suggested a change in the contact state. This trend was consistent with the results of the study by Petean and Aguiar [10]. Therefore, it was important to set the initial load on the particles in the centrifugal method to evaluate the actual phenomenon.

No significant differences in the effective contact radius were observed within the range of the initial load in this experiment. Presumably, the initial load did not generate a sufficiently large change to alter the particle orientation. Therefore, only minor changes were observed in the contact region.

5. Summary and conclusions

In this study, we performed experiments to remove spherical particles adhering to horizontal and vertical substrates by using a centrifuge with a vertical axis of rotation. The particles were glass beads with D_{p50} of 9.7, 14.5, and 32.8 μm. Additionally, the adhesion force between the particles and substrate and effective contact radius were obtained by formulating and combining the moments of force exerted on the particles on the horizontal and vertical substrates.

The conclusions of the study are as follows:

1. The centrifugal force required to remove the particles increased as particle diameter increased.
2. The centrifugal force required to remove the particles from a horizontal substrate was significantly lower than that from a vertical substrate. This suggests that particle rolling plays a crucial role in the removal mechanism.
3. For each particle sample, two angular velocities relating to the same removal fraction were obtained in experiments using vertical and horizontal substrates. These were substituted in simultaneous equations. Hence, the adhesion strength distribution corresponding to removal fractions was obtained. Additionally, it was quantitatively shown that the adhesion force increased significantly as particle diameter increased.
4. The effective contact radius was not affected by the removal fraction but increased with increasing particle diameter. The contact radius between the surface of the smooth substrate (R_a < 1 nm) and particle with D_{p50} = 32.8 μm corresponded to 0.5 μm.
5. The adhesion force was lower, and the effective contact radius was higher for a substrate with a rough surface (R_a = 33 nm).
6. The adhesion force increased as relative humidity ($\varphi \leq 72\%$) and initial load on the particle ($F_0 \leq 4.1$ μN) increased. However, they did not affect the effective contact radius.

Declaration of Competing Interest

None.

References

[1] Y. Shimada, Y. Yonezawa, H. Sunada, Measurement and evaluation of the adhesive force between particles by the direct separation method, J. Pharm. Sci. 92 (2003) 560–568, https://doi.org/10.1002/jps.10313.

[2] S. Matsusaka, D. Wei, M. Yasuda, S. Sasabe, Adhesive strength distribution of charged particles on metal substrate in external electric field, Adv. Powder Technol. 26 (2015) 149–155, https://doi.org/10.1016/j.apt.2014.08.017.

[3] Y. Kato, M. Ohkuma, Y. Shimada, H. Sunada, Evaluation of the flowability of surface-modified preparations by the measurement of the inter-particle adhesive force, J. Drug Deliv. Sci. Technol. 15 (2005) 217–221, https://doi.org/10.1016/S1773-2247(05)50035-2.

[4] Y. Yanbin, S. Matsusaka, H. Hiroaki, T. Toyokazu, Characterizing the effect of surface morphology on particle–wall interaction by the airflow method, Adv. Powder Technol. 17 (2006) 413–424, https://doi.org/10.1163/156855206777866119.

[5] K. Higashitani, H. Makino, S. Matsusaka, Powder Technology Handbook, fourth ed CRC Press, 2020 113–120.

[6] W.A. Ducker, T.J. Senden, R.M. Pashley, Direct measurement of colloidal forces using an atomic force microscope, Nature. 353 (1991) 239–241, https://doi.org/10.1038/353239a0.

[7] JIS, Z 8845, Determination of particle adhesion force by centrifugal method, 2021.

[8] H. Mizes, M. Ott, E. Eklund, D. Hays, Small particle adhesion: measurement and control, Colloid Surface A 165 (2000) 11–23, https://doi.org/10.1016/S0927-7757(99)00442-2.

[9] G.R. Salazar-Banda, M.A. Felicetti, J.A.S. Gonçalves, J.R. Coury, M.L. Aguiar, Determination of the adhesion force between particles and a flat surface, using the centrifuge technique, Powder Technol. 173 (2007) 107–117, https://doi.org/10.1016/j.powtec.2006.12.011.

[10] P.G.C. Petean, M.L. Aguiar, Determining the adhesion force between particles and rough surfaces, Powder Technol. 274 (2015) 67–76, https://doi.org/10.1016/j.powtec.2014.12.047.

[11] C.A. Stevenson, M.C. Thomas, S.P. Beaudoin, An enhanced centrifuge-based approach to powder characterization: the interaction between particle roughness and particle-scale surface topography described by a size-dependent 'effective' Hamaker constant, Powder Technol. 391 (2021) 198–205, https://doi.org/10.1016/j.powtec.2021.06.006.

[12] F. Podczeck, J.M. Newton, Development of an ultracentrifuge technique to determine the adhesion and friction properties between particles and surfaces, J. Pharm. Sci. 84 (1995) 1067–1071, https://doi.org/10.1002/jps.2600840907.

[13] H.-C. Wang, Effects of inceptive motion on particle detachment from surfaces, Aerosol Sci. Technol. 13 (1990) 386–393, https://doi.org/10.1080/02786829008959453.

[14] S. Matsusaka, M. Koumura, H. Masuda, Analysis of adhesive force between particle and wall based on particle reentrainment by airflow and centrifugal separation, Kagaku Kogaku Ronbun. 23 (1997) 561–568, https://doi.org/10.1252/kakoronbunshu.23.561.

[15] K. Ilse, M.Z. Khan, K. Lange, H.N. Gurumoorthy, V. Naumann, C. Hagendorf, J. Bagdahn, Rotational force test method for determination of particle adhesion—from a simplified model to realistic dusts, J. Renew. Sustain. Ener. 12 (2020) 15122, https://doi.org/10.1063/5.0015122.

[16] K.V. Aracena, R.O. Unac, I. Ippolito, Vidales, Movement initiation of millimeter particles on a rotating rough surface: the role of adhesion, Particuology 53 (2020) 92–99, https://doi.org/10.1016/j.partic.2020.02.004.

[17] J. Czarnecki, T. Dąbroś, Attenuation of the van der Waals attraction energy in the particlesemi-infinite medium system due to the roughness of the particle surface, J. Colloid Interface Sci. 78 (1980) 25–30, https://doi.org/10.1016/0021-9797(80)90491-9.

[18] J. Charnecki, V. Itschenskij, Van der Waals attraction energy between unequal rough spherical particles, J. Colloid Interface Sci. 98 (1984) 590–591, https://doi.org/10.1016/0021-9797(84)90189-9.

[19] J. Israelachvili, Intermolecular and Surface Forces, Academic Press, 2011 456–460.